Hindawi
Complexity
Volume 2020, Article ID 5409401, 13 pages
https://doi.org/10.1155/2020/5409401

Research Article

Containing Epidemic Spreading on Networks with Neighbor Resource Supporting

Chengcheng Song,[1] Yanyan Chen,[1] Ning Chen,[1] Zhuo Liu,[1] Xuzhen Zhu,[2] and Wei Wang[3]

[1]*Beijing Key Laboratory of Traffic Engineering, Beijing University of Technology, Beijing 100124, China*
[2]*State Key Laboratory of Networking and Switching Technology, Beijing University of Posts and Telecommunications, Beijing 100876, China*
[3]*Cybersecurity Research Institute, Sichuan University, Chengdu 610065, China*

Correspondence should be addressed to Yanyan Chen; cdyan@bjut.edu.cn and Ning Chen; chenningscut@126.com

Received 20 July 2020; Revised 23 October 2020; Accepted 16 November 2020; Published 30 November 2020

Academic Editor: Honglei Xu

Previous studies revealed that the susceptibility, contacting preference, and recovery probability markedly alter the epidemic outbreak size and threshold. The recovery probability of an infected node is closely related to its obtained resources. How to allocate limited resources to infected neighbors is extremely important for containing the epidemic spreading on complex networks. In this paper, we proposed an epidemic spreading model on complex networks, in which we assume that the node has heterogeneous susceptibility and contacting preference, and susceptible nodes are willing to share their resources to neighbors. Through a developed heterogeneous mean-field theory and a large number of numerical simulations, we find that the recovered nodes provide resources uniformly to their infected neighbor nodes, and the epidemic spreading can be suppressed optimally on homogeneous and heterogeneous networks. Besides, altering the susceptibility and contacting preference does not qualitatively change the results. The susceptibility of the node decreases, which makes the outbreak threshold of epidemic spreading increase, and the outbreak size decreases. Our theory agrees well with the numerical simulations.

1. Introduction

Extensive phenomena, such as infectious disease spreading, information diffusion, and rumor propagation, in real-world systems, can be described as "epidemic" spreading on complex networks [1–5]. In such a description framework, nodes represent elements and edges stand for the relationship among nodes. Previous studies have revealed that the evolution mechanisms, network topology, and social factors are markedly affecting the epidemic outbreak size and threshold point [6–12]. Researchers found that strong degree heterogeneity makes the outbreak threshold vanish [6]. When epidemic spreading dynamics on multilayer networks, the system may exist a hybrid phase transition; that is to say, the epidemic outbreaks globally in one network and spreads locally in the other network [13–20]. Davis et al. proposed a Maki–Thompson rumor-spreading model on multipopulations and found that the dynamical behaviors and threshold are closely correlated to the interactions between spreading and subpopulations [21].

Designing effective strategies for fast recovery infected nodes is extremely important for epidemic spreading. On the one hand, researchers investigated the effects of recovery probability on epidemic spreading, including the epidemic outbreak size and threshold. Shu et al. [22] investigated the recovery probability on the classical susceptible-infected-recovered (SIR) model, by using an edge-based compartmental theory and synchronous updating numerical simulations, and they found that the outbreak threshold increases with the recovery probability for a given effective infection probability. For epidemic spreading dynamics with general recovery probability, the dynamic always exhibits a non-Markovian character, which makes the theoretical predictions deviate from the numerical simulations [23–27].

Karrer and Newman [28] proposed a general message-passing approach for epidemic spreading with a general recovery probability distribution and markedly agree with numerical simulations. de Arruda and his colleagues [29] studied the roles of heterogeneous recovery probability and revealed that the critical infectivity is smaller than the values predicted by the quenched mean-field approaches.

On the other hand, researchers revealed that resources (e.g., masks and specific drugs) are an essential factor for epidemic recovery [30]. How to allocate the resources to individuals is important. Chen et al. [31] assumed that the recovery probability of infected nodes depends on the amount of received resources. Through a mean-field theory, they found that the system exhibits a discontinuous phase transition when the resources are insufficient. They further consider the resource allocation correlates to a social network, and they investigated the effects of different resource allocation strategies, network topologies, interlayer degree-degree correlations on the epidemic spreading, and phase transition [32–35]. By using extensive numerical Monte-Carlo simulations and the message-passing approach, they revealed that the phase transition closely correlated to those essential factors. Recently, Zhang et al. [36] revealed an optimal resource allocation strategy, at which the epidemic will be significantly suppressed.

In reality, distinct individuals always have different susceptibility, inelastic resources (e.g., time), and medical resources (e.g., masks). When a pandemic epidemic is spreading, such as SARS and COVID-19, the above three factors are essential. Neglecting any one may lead to a misunderstanding about the spreading dynamics. To our best knowledge, there is still a lack of a mathematical model, which includes the three aspects simultaneously. Specifically, we will propose a generalized SIR epidemic spreading dynamics considering the following three aspects. (i) Each node with an inherent infection threshold is used to reflect the susceptibility of nodes. The larger the values of infection threshold, the smaller the susceptibility. Miller [37] revealed that an epidemic is a more likely outbreak for homogeneous infectivity. Watts [38] revealed that the phase transition is discontinuous when the infection threshold is included. (ii) We preferred contact with neighbors due to the limited energy and time. Previous studies found that preferring contacting nodes with small degrees promotes the spreading dynamics [39, 40]. (iii) The resource supporting is determined by the degree of nodes. We propose an epidemic spreading dynamic on complex networks, including the above three aspects simultaneously, and discuss the effects of the above three aspects of epidemic spreading dynamics.

The organization of this paper as follows: in Section 2, we describe our model. In Section 3, we develop a heterogeneous mean-field theory to describe the spreading dynamics. The numerical simulations are performed in Section 4. Finally, we draw the conclusions in Section 5.

2. Model Descriptions

In this section, we describe the epidemic spreading dynamics model on complex networks.

2.1. Network Description. To describe the complex networks, we adopt two types of artificial networks: ER network and uncorrelated configuration networks. We denoted the network size, degree distribution, and average degree as N, $P(k)$, and $\langle k\rangle = \sum_k kP(k)$, respectively. To build the ER network, two nodes are connected with probability p. Therefore, we have $\langle k\rangle = pN$. For the uncorrelated configuration networks, we build as follows: (i) assign the values of N and $P(k)$. Specifically, we assume the degree distribution follows a power-law distribution $P(k) = \zeta k^{-\gamma_D}$, where $\zeta = 1/\sum_k k^{-\gamma_D}$, γ_D represents the degree exponent. The larger of γ_D, the homogeneous of the degree distribution. (ii) Assign degree for each node according to $P(k)$. (iii) Assign stubs for each node, and the number of stubs equals to its degree. (iv) Randomly connect two stubs to build an edge. Note that we disallow multiple edges and self-loops. (v) Repeat step (iv) until there are no stubs left. The pseudocode of building the uncorrelated configuration networks is shown in Algorithm 1 [41].

2.2. Epidemic Spreading Model. To describe the epidemic spreading dynamics on complex networks, we adopt a generalized susceptible-infected-recovered (SIR) model. A susceptible node represents that the epidemic does not infect it. Infected node stands for that it is infected by the epidemic and can transmit the epidemic to susceptible neighbors. Recovered nodes means that it is ever infected by the epidemic and recovered. Note that the recovered nodes will not participate in the remaining spreading dynamics. The immune system response, such as allergic response, is dependent on multiple exposures [42]. For the case of social contagions, an individual should eliminate the adoption risk before adopting a product, innovation, or behavior. Therefore, multiple exposures are needed [43, 44]. To include this essential factor, we assume that every node has an inherent infectious threshold f to reflect the fraction of exposures that a susceptible node should have before become an infected node.

The epidemic spreading dynamics evolves as follows. Initially, randomly select a fraction of s nodes as the seeds (i.e., in the infected state), and the remaining nodes are set to be in the susceptible state. At each time interval $t + \delta t$, every infected node i tries to transmit the infection to a neighbor according to some strategies. Since every individual has limited time and energy, he always preferentially contact some neighbors to transmit the infection. We here assume that node i selects node j to transmit the infection with probability:

$$p_{ij} = \frac{k_j^\beta}{\sum_{j\in\Omega(i)} k_j^\beta}, \tag{1}$$

where $\Omega(i)$ represents the neighbor set of node i. The parameter β is used to reflect the preference of contacting. For the case of $\beta < 0$, the infected node prefers to select neighbors with a small degree. The opposite situation happens when $\beta > 0$. For the case of $\beta = 0$, the infected node contacts neighbors randomly. If node j is in the infected or recovered state, nothing happens. If node j is in the susceptible state,

(1) Input: N and $P(k)$
(2) Output: Network G
(3) Assigning degree k_i for each node i according to $P(k)$
(4) Assigning stubs ℓ_i for each node with same value of degree k_i, i.e., $\ell_i = k_i$
(5) **while** $h = \sum_i \ell_i > 0$ **do**
(6) Randomly select two stubs m and $n \neq m$ to build an edge e_{mn}
(7) $h \longleftarrow h - 2$
(8) **end while**

Algorithm 1: Building uncorrelated configuration networks.

node i transmits the infection to node j with probability $\lambda \delta t$. The number of infections y_j is that node j plus one, i.e., $y_j = y_j + 1$. If $y_j \geq \lceil f k_j \rceil$, node j becomes infected, where k_j is the degree of node j and $\lceil x \rceil$ means ceil of x.

The recovery of infected nodes always needs some resources from public resources and friends' support. In this paper, we focused on the latter one and assumed that every susceptible node is generous and willing to share resources with neighbors. The number of resources of nodes is always related to their inherent characteristics (e.g., age, profession and education), which can be reflected by their degrees to some extent. The simplest way to describe the individuals' characteristics is by using their degrees. Therefore, we assume that a susceptible node u with degree k_u provides k_u^α pieces of resources. For the case of $\alpha > 0$, nodes with a large degree can provide more resources. The opposite situation happens when $\alpha < 0$. For the case of $\alpha = 0$, all nodes provide the pieces of the resource. To normalize the resources, we set a susceptible node u can provide $k_u^\alpha / \max\{k_{\min}^\alpha, k_{\max}^\alpha\}$ resources, where $k_{\min}$ and $k_{\max}$ represent the minimum and maximum degrees, respectively. Therefore, the infected node i receives r_i pieces of resources and can be expressed as

$$r_i = \sum_{u \in \Gamma(i)} \frac{k_u^\alpha}{\max\{k_{\min}^\alpha, k_{\max}^\alpha\}}. \tag{2}$$

With r_i pieces of resources, $\Gamma(i)$ is the set of susceptible neighbors of node i, and the infected node i becomes recovered with rate:

$$\mu_i = 1 - (1 - \mu_0)^{w r_i} + \mu_1, \tag{3}$$

where μ_0 is the basic recovery probability with one piece of resource. w is the resource utilization, and μ_1 is endogenous probability. The spreading dynamics terminates when there are no nodes in the infected state. In the final state, the epidemic spreading size R is the fraction of nodes in the recovered state. The pseudocode of the spreading dynamics is presented in Algorithm 2.

The model proposed in this section includes three important aspects: (i) we use an inherent infection threshold to describe the heterogeneous susceptibility of nodes, which is similar to the threshold model, (ii) we preferentially contact neighbors according to equation (1), and (iii) the recovery probability is determined by equation (3).

3. Theoretical Analysis

To describe the epidemic spreading dynamics on complex networks, we here use a heterogeneous mean-field theory inspired by [6]. In this theory, we make the following three assumptions: (i) nodes with the same values of degrees have the same statistical properties, and (ii) the infected neighbors, e.g., node u and v, of a susceptible node i transmit the infection to node i independently. That is to say, we neglect the dynamical correlations among the states of neighbors. (iii) In theory, we assume the epidemic spreading on large-scale systems.

3.1. Evolution Dynamics. Denoting $S_k(t)$, $I_k(t)$, and $R_k(t)$ as the probability that a randomly selected node with degree k at time t is in the susceptible, infected, and recovered state, respectively. Since at very time step, a node should be in one of the three states, we have

$$S_k(t) + I_k(t) + R_k(t) = 1. \tag{4}$$

In what follows, we will derive the evolutions of $S_k(t)$, $I_k(t)$, and $R_k(t)$.

For a susceptible node u with degree k, the probability that u is in the susceptible state decreases when u is infected by neighbors. From the descriptions in Section 2, we know that node u infected by neighbors at time t should fulfill a situation; that is to say, node u at least received $\lceil fk \rceil$ infections from neighbors. We denote $\theta_k(t)$ as the probability that a susceptible node with degree k receives one piece of infection from a neighbor. Therefore, the probability that node u receives m pieces of infections from neighbors is

$$\varphi_k(t) = \binom{k}{m} [\theta_k(t)]^m [1 - \theta_k(t)]^{k-m}. \tag{5}$$

We further get that probability that node u becomes infected at time t with probability:

```
(1) Input: Network G and dynamical parameters λ, μ1, μ0, w, α, β, f, ρ0;
(2) Output: Epidemic spreading size R;
(3) Randomly selecting ρ0 seeds, and put them into queue Q1;
(4) t ⟵ 0;
(5) Initialize yj for every node j;
(6) while Q1 is not empty do
(7)    Initialize Q2 to be empty;
(8)    δt ⟵ 1/length(Q1);
(9)    for i = 1 to length(Q1) do
(10)      Node i of Q1 selects one neighbor j to contact according to equation (1);
(11)      Node i transmits the infection to node j with probability λδt if j is in the susceptible state;
(12)      if Node j receives the infection from i then yj←yj + 1
(13)      end if
(14)      if yj ≥ ⌈fkj⌉ then
(15)         Node j becomes infected, and put it into queue Q2;
(16)      end if
(17)   end for
(18)   for i = 1 to length(Q1) do
(19)      Recovering node i according to equation (3);
(20)      if Node i recovers then
(21)         Delete node i from queue Q1;
(22)      end if
(23)   end for
(24)   for i = 1 to length(Q2) do
(25)      Adding node i to queue Q1;
(26)      Deleting node i from queue Q2;
(27)   end for
(28)   t←t + δt
(29) end while
```

Algorithm 2: Epidemic spreading dynamics.

$$\Psi_k(t) = S_k(t) \sum_{m=\lceil fk \rceil}^{k} \varphi_k(t). \tag{6}$$

By using equations (5) and (6), we can describe the infection threshold in our model. The evolution of $S_k(t)$ is

$$\frac{dS_k(t)}{dt} = -\Psi_k(t). \tag{7}$$

Until now, we do not know the value of $\theta_k(t)$.

To obtain $\theta_k(t)$, we should compute the following three aspects:

(i) The probability of node u connects to an infected neighbor node v with degree k'. In uncorrelated network, we know the probability that an edge of node u connects to node v is $k'P(k')/\langle k\rangle$, where $\langle k\rangle$ is the average degree of the network.

(ii) The infected node v selects node u to contact according to equation (1). The weight of node v selecting node u is k^β. The weight of remaining $k'-1$ neighbors is $H(k'-1)$, where H is the average weight of node v selecting one node to contact except for node u, and it is expressed as

$$\begin{aligned} H &= \sum_{k''} \frac{k''P(k'')}{\langle k\rangle} (k'')^\beta \\ &= \frac{\langle k^{\beta+1}\rangle}{\langle k\rangle}, \end{aligned} \tag{8}$$

where $\langle k^{\beta+1}\rangle$ is the $\beta+1$-th moment of the degree distribution. Therefore, the preferred contact probability that node v selects node u to contact is

$$G(k,k') = \frac{k^\beta}{H(k'-1) + k^\beta}. \tag{9}$$

(iii) Node v successfully transmits the infection to node u with probability λ. Combining the above three aspects, we obtain

$$\theta_k(t) = \lambda\left[\sum_{k'} \frac{k'P(k')}{\langle k\rangle} G(k,k') I_{k'}(t)\right]. \tag{10}$$

Inserting equation (10) into equation (7), we get the evolution of $S_k(t)$.

For the evolution of $I_k(t)$, we should consider two aspects. On the one hand, the susceptible node u with degree k becomes infected with the probability $\Psi_k(t)$, which induces the increase of $I_k(t)$. On the other hand, the infected nodes with degree k become recovered μ_k, which causes the decrease of $I_k(t)$. The expression of μ_k is

$$\mu_k = 1 - (1-\mu_0)^{w\phi_k} + \mu_1, \tag{11}$$

where ϕ_k is the pieces of resources that node v receives from neighbors. According to equation (2), we know

$$\phi_k = (k-1)\sum_{k'} \frac{k'P(k')}{\langle k\rangle} S_{k'}(t) \frac{k'^{\alpha}}{\max\{k_{\min}^{\alpha}, k_{\max}^{\alpha}\}}. \tag{12}$$

On the right hand of equation (12), we times $k-1$ since an infected node v must connect to an infected neighbor. By using equations (11) and (12), the recovery probability can be computed. Therefore, we get the evolution of $I_k(t)$ as

$$\frac{dI_k(t)}{dt} = \Psi_k(t) - \mu_k I_k(t). \tag{13}$$

The evolution of $R_k(t)$ is

$$\frac{dR_k(t)}{dt} = \mu_k I_k(t). \tag{14}$$

Combining equations (7), (13), and (14), we can get the fraction of nodes in the susceptible, infected, and recovered state as

$$X(t) = \sum_{k=1}^{k_{\max}} P(k) X_k(\infty), \tag{15}$$

where $X \in \{S, I, R\}$. When $t \longrightarrow \infty$, the epidemic outbreak size is

$$R(\infty) = \sum_{k=1}^{k_{\max}} P(k) R_k(\infty). \tag{16}$$

3.2. Threshold Analysis. In what follows, we study the threshold point λ_c of the system. Previous studies indicated that when $\lambda \le \lambda_c$, the global epidemic spreading is impossible. Otherwise, when $\lambda > \lambda_c$, the global epidemic outbreak becomes possible. Initially, we only randomly a vanishingly small fraction of seeds. Thus, we have $I_k(0) \approx 0$, $S_k(0) \approx 1$, and the high order of $I_k(t)$ can be neglected when $t \longrightarrow 0$. Rewriting equation (13) and neglecting the high orders of $O(I_k(t)^2)$, when $\lceil fk \rceil = 1$, we have

$$\begin{aligned}
\frac{dI_k(t)}{dt} &= \Psi_k(t) - \mu_k I_k(t) \\
&= S_k(t)\left\{1 - \sum_{m=0}^{\lceil fk\rceil - 1} \binom{k}{m} [\theta_k(t)]^m [1-\theta_k(t)]^{k-m}\right\} \\
&\quad - \left[1 - (1-\mu_0)^{w\phi_k} + \mu_1\right] I_k(t) \\
&\approx k\theta_k(t) - (\mu_0 w\phi_k + \mu_1) I_k(t) \\
&\approx k\lambda\left[\sum_{k'} \frac{k'P(k')}{\langle k\rangle} G(k,k') - \delta_{kk'}\left(\mu_0 w\widetilde{\phi}_k + \mu_1\right)\right] I_{k'}(t),
\end{aligned} \tag{17}$$

where $\delta_{kk'} = 1$ only when $k = k'$, and $\widetilde{\phi}_k = (k-1)\sum_{k'}((k'P(k'))/\langle k\rangle)(k'^{\alpha}/(\max\{k_{\min}^{\alpha}, k_{\max}^{\alpha}\}))$. Rewriting equation (17), we have

$$\frac{d\overrightarrow{I}(t)}{dt} = \mathscr{L}'\overrightarrow{I}(t), \tag{18}$$

where $\overrightarrow{I}(t) = \left\{I_{k_{\min}}(t), \ldots I_{k_{\max}}(t)\right\}^T$ and $\mathscr{L}'_{kk'} = k\lambda[\sum_{k'}((k'P(k'))/\langle k\rangle)G(k,k') - \delta_{kk'}(\mu_0 w\widetilde{\phi}_k + \mu_1)]$.

In a similar way, we study the case of $\lceil fk \rceil > 1$. We have

$$\frac{d\overrightarrow{I}(t)}{dt} = \mathscr{L}''\overrightarrow{I}(t), \tag{19}$$

where $\mathscr{L}''_{kk'} = (2k - k^2)\lambda[\sum_{k'}((k'P(k'))/\langle k\rangle)G(k,k') - \delta_{kk'}(\mu_0 w\widetilde{\phi}_k + \mu_1)]$. Combining the above two cases, we have

$$\frac{\mathrm{d}\overrightarrow{I}(t)}{\mathrm{d}t} = \mathscr{L}\overrightarrow{I}(t), \tag{20}$$

where

$$\mathscr{L}_{kk'} = \begin{cases} \mathscr{L}'_{kk'}, & \text{if } \lceil fk \rceil = 1, \\ \mathscr{L}''kk', & \text{otherwise.} \end{cases} \tag{21}$$

According to the stability analysis in [45], we know the global epidemic outbreak only when the largest eigenvalue $\Lambda_1(\mathscr{L})$ of $\mathscr{L}$ is larger than 0. Otherwise, the global epidemic outbreak is very small. The critical epidemic transmission probability λ_c fulfills

$$\Lambda_1(\mathscr{L}) = 0. \tag{22}$$

4. Simulation Results and Analysis

We perform a large number of numerical simulations on the Erdös–Rényi (ER) and scale-free (SF) networks with network size $N = 10^4$, and average degree $\langle k\rangle = 10$. The basic recovery probability is $\mu_0 = 0.1$, the endogenous recovery is $\mu_1 = 0.1$, the resource utilization is $w = 0.1$, and the initial seed ratio $\rho_0 = 0.0005$. By performing extensive numerical simulations, we found that other values of μ_0, μ_1, and w do not qualitatively affect the results presented in this paper. Through a large number of theoretical analysis and experimental simulation, we find that other parameters change the conclusion presented in this paper qualitatively. All results presented in this paper are averaged at least 1000 times on 10 different networks.

On the ER network, we first study the variation of the outbreak size $R(\infty)$ with the transmission probability λ with different preference selection parameters β as shown in Figure 1. It can be found from Figure 1(a) that as the transmission probability increases, the probability of susceptible nodes gets the infection increased; thus, the outbreak size also increases. The outbreak size decreases first and then increases with the resource provision parameter α. Specifically, when λ is the same, the outbreak size corresponding to $\alpha = -0.5$ is the largest, the outbreak size of $\alpha = 0.5$ is between three α values, and the smallest size is among the three α values when $\alpha = 0.0$, while the outbreak threshold increases first and then decreases with the resource provision parameter α according to equation (22). Specifically, the outbreak threshold corresponding to $\alpha = -0.5$ is the smallest, the outbreak threshold of $\alpha = 0.5$ is between three α values, and the largest size is among the three α values when $\alpha = 0.0$. Therefore, there is α_{opt} at which outbreak size $R(\infty)$ is the smallest and outbreak threshold is the largest (to be detailedly discussed in Figure 2). We can understand the above phenomena as follows. For the case of $\alpha = 0.0$, a susceptible node j provides a piece of resource to its infected neighbor i. For other values of α, the node j at most provides one piece of resource to node i. In this situation, node i receives the maximum resources $r_i = |\Gamma_i|$ when $\alpha = 0.0$, where $|\Gamma_i|$ is the number of the set Γ_i. Therefore, node i has the largest recovery probability when $\alpha = 0.0$.

Three peak values of Δ in Figure 1(d) represent the simulated outbreak threshold for $\alpha = -0.5$, $\alpha = 0.0$, and $\alpha = 0.5$, respectively. Δ is obtained through variability calculation, and the calculation formula is [46]

$$\Delta = \frac{\sqrt{\langle R(\infty)^2\rangle - \langle R(\infty)\rangle^2}}{\langle R(\infty)\rangle}. \tag{23}$$

They correspond to the arrows in Figure 1(a) representing the theoretical outbreak threshold. It can be seen that the theoretical prediction of $R(\infty)$ and theoretical outbreak threshold well agree with the numerical predictions. The reason for the deviation between the theoretical and simulation results is the strong correlation between the neighbor state and the finite size network. The most important thing is that we found that changing the value of β did not qualitatively change the above results. The numerical simulation results are good agreement with the theoretical predictions.

In Figures 3 and 4, we study the effects of different values of f on the epidemic spreading dynamics. With the increase of f, the epidemic outbreak threshold increases and the epidemic outbreak size decreases. Different from previous studies [38], in which the phase transition is discontinuous when the infection threshold is large enough, we find that $R(\infty)$ always increases continuously with λ regardless of f. We explain the result as follows. In our model, an infected node's contact ability is limited; that is, an infected node only contacts one neighbor to transmit the infection. In this situation, the susceptible state node becomes infected gradually and cannot induce a finite fraction of susceptible nodes becoming infected state simultaneously. Thus, $R(\infty)$ increases with λ continuously. In addition, we also observed a phenomenon similar to Figure 1. Specifically, when the propagation probability λ is the same, the outbreak size $R(\infty)$ reaches the minimum when $\alpha = 0.0$ and the outbreak threshold reaches the maximum when $\alpha = 0.0$. That is, there is also an optimal α value here. Above all, from Figures 1, 3, and 4, we can see that the change in f value has no effect on $\alpha_{\mathrm{opt}} = 0.0$, and α_{opt} always exists, since the recovery probability reaches the maximum value at α_{opt}. Next, it will be systematically discussed and studied.

In Figure 2, we explore the effects of α and λ on the epidemic spreading on ER networks. From Figures 2(a)–2(c), we observe that when $\alpha < 0$, the $R(\infty)$ decreases with α while $\alpha > 0$ and increases with α. The variation of the outbreak threshold is opposite to the outbreak size. When $\alpha < 0$, the outbreak threshold increases with α while $\alpha > 0$ and decreases with α. Therefore, there is an optimal value $\alpha_{\mathrm{opt}} = 0$, i.e., white dotted line, where $R(\infty)$ reaches the minimum value, and λ_c is the largest. Because when $\alpha = 0$, the volume of resources received by the infected nodes for recovery is the largest, which makes them become recovered quickly. The value of the parameter β does not qualitatively change the above phenomena. We also mainly realized that the change of the parameter f cannot qualitatively change these phenomena, but the increase of f can reduce the

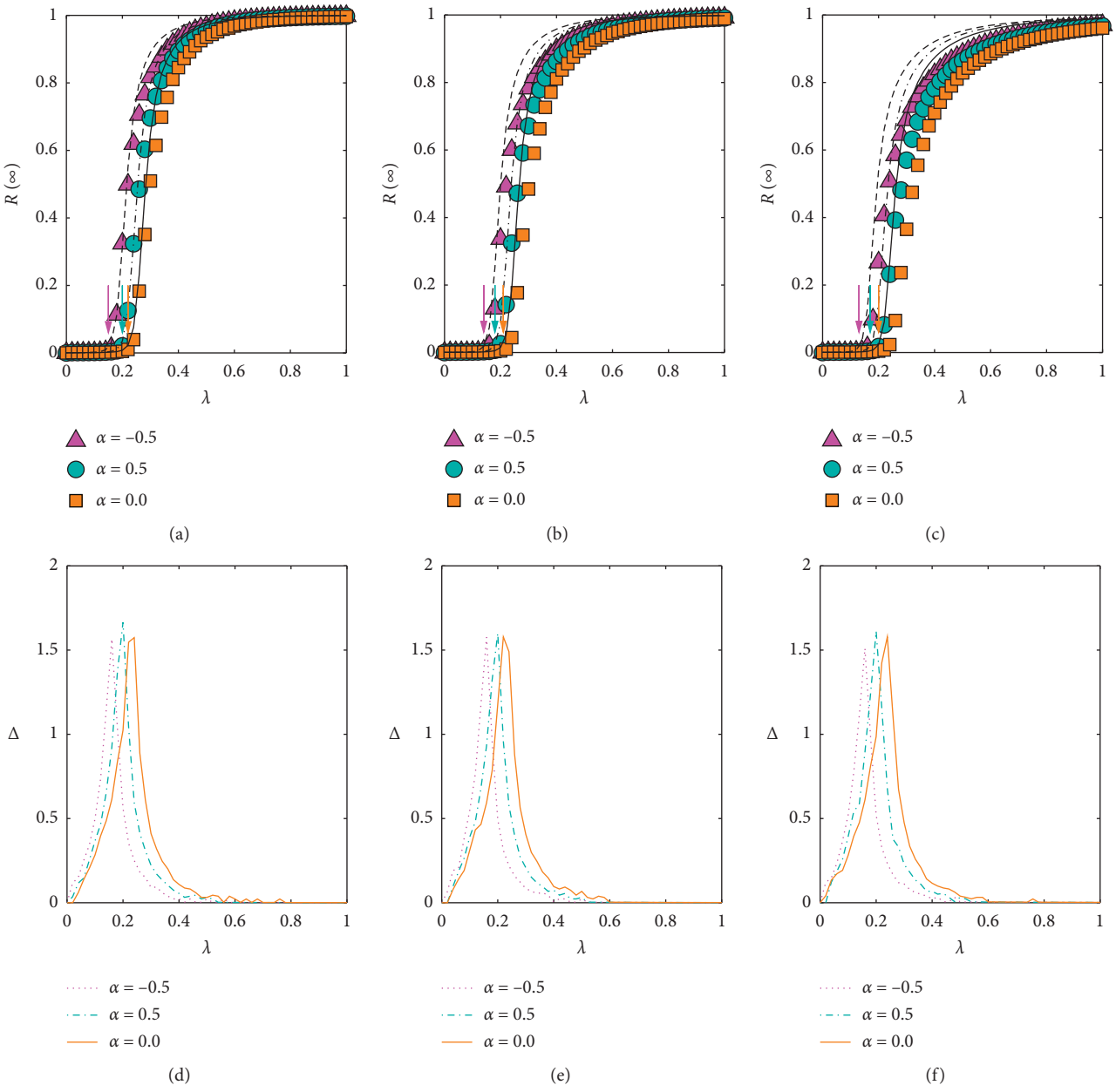

FIGURE 1: The variation of the outbreak size $R(\infty)$ with the transmission probability λ with different preference selection parameters β. (a) ($\beta = -1$), (b) ($\beta = 0$), and (c) ($\beta = 1$). The symbols and lines are the simulated and theoretical values of $R(\infty)$ in (a)–(c), respectively, where $\alpha = -0.5$ (pink triangles), $\alpha = 0.0$ (orange squares), and $\alpha = 0.5$ (blue-green circles). The arrows are theoretical outbreak threshold. The simulated outbreak threshold Δ as a function of λ with $\beta = -1$ (d), $\beta = 0$(e), and $\beta = 1$ (f) for the corresponding values of α in (a)–(c), respectively. Another parameter is $f = 0.03$.

outbreak size and increase the outbreak threshold, which is the same as the conclusion obtained in Figures 1, 3, and 4.

We further research the effects of λ and α on spreading dynamics on SF networks with power-law degree distribution $P(k) = ck^{-\gamma}$, where γ is the degree distribution exponent and $c = 1/\sum_k k^{-\gamma}$, and the maximum degree is set as $k_{\max} \sim \sqrt{N}$. The simulations are performed on a strong heterogeneity network with $\gamma = 3$. We plot the phase diagram of the theoretical outbreak size $R(\infty)$ as a function of α and λ on the SF network with different values of β in Figure 5. We find similar phenomena in Figure 2. Specifically, in Figures 5(a)–5(c), for $\alpha < 0$, the $R(\infty)$ decreases with α and outbreak threshold increases with α. For $\alpha > 0$, the $R(\infty)$ increases with α and outbreak threshold decreases with α. Thus, there is an optimal value of α that makes $R(\infty)$ is the smallest, and the outbreak threshold is the largest, i.e., $\alpha_{\text{opt}} = 0$. The explanation of this optimal phenomenon is the same as that on the ER network of Figure 2. No matter how the values of β and f change, the optimal value of α will not disappear. As f increases, the final outbreak size decreases, and the outbreak threshold increases. The theoretical and simulation results agree well.

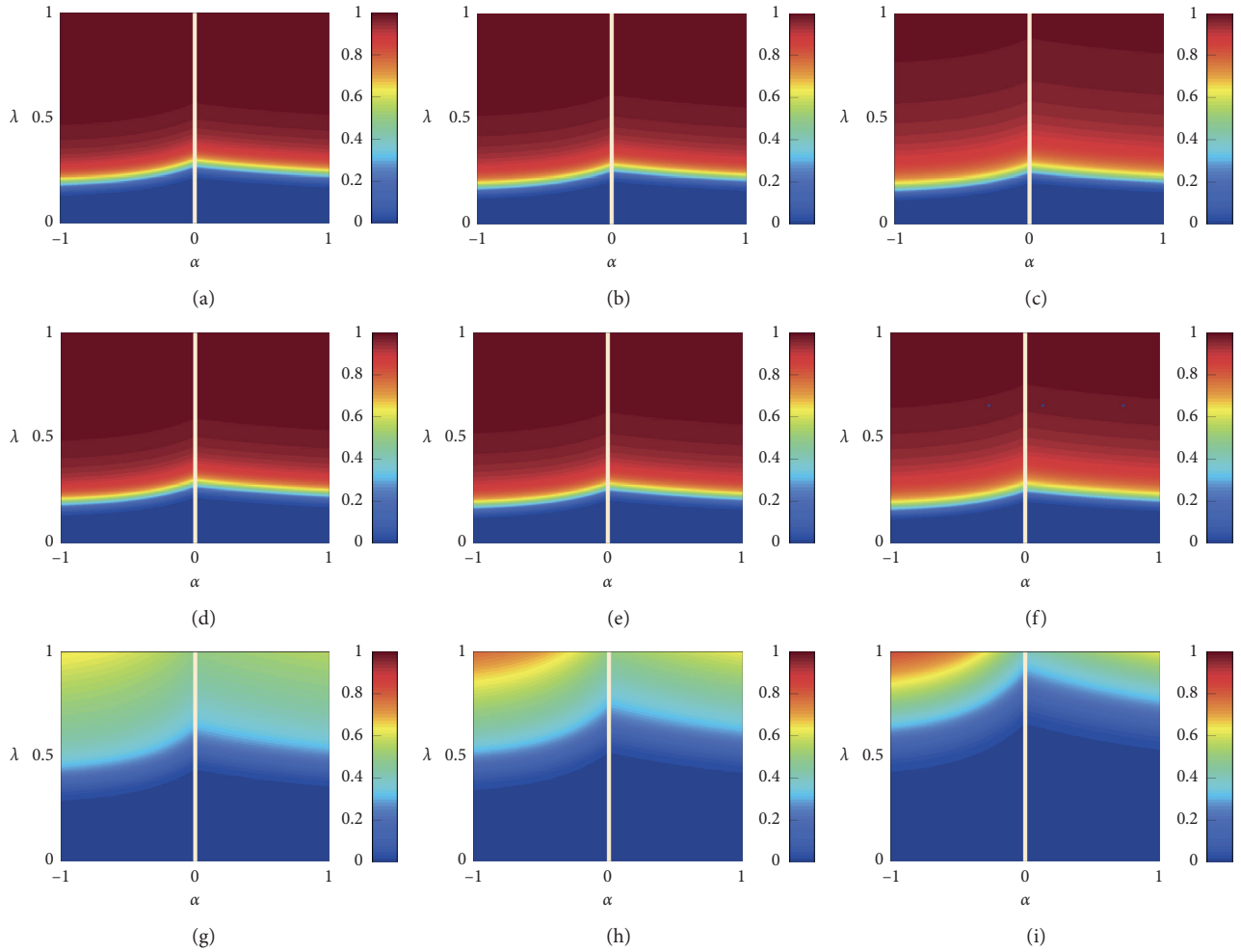

Figure 2: Phase diagram on parameter space (α, λ) on the ER network with $\beta = -1$ (a) (d) (g), $\beta = 0$ (b) (e) (h), and $\beta = 1$ (c) (f) (i). (a)–(c) ($f = 0.03$), (d)–(f) ($f = 0.05$), and (g)–(i) ($f = 0.1$). The color represents the theoretical value of the outbreak size $R(\infty)$. The white dotted line in each subgraph indicates the optimal value of $\alpha_{\text{opt}} = 0$.

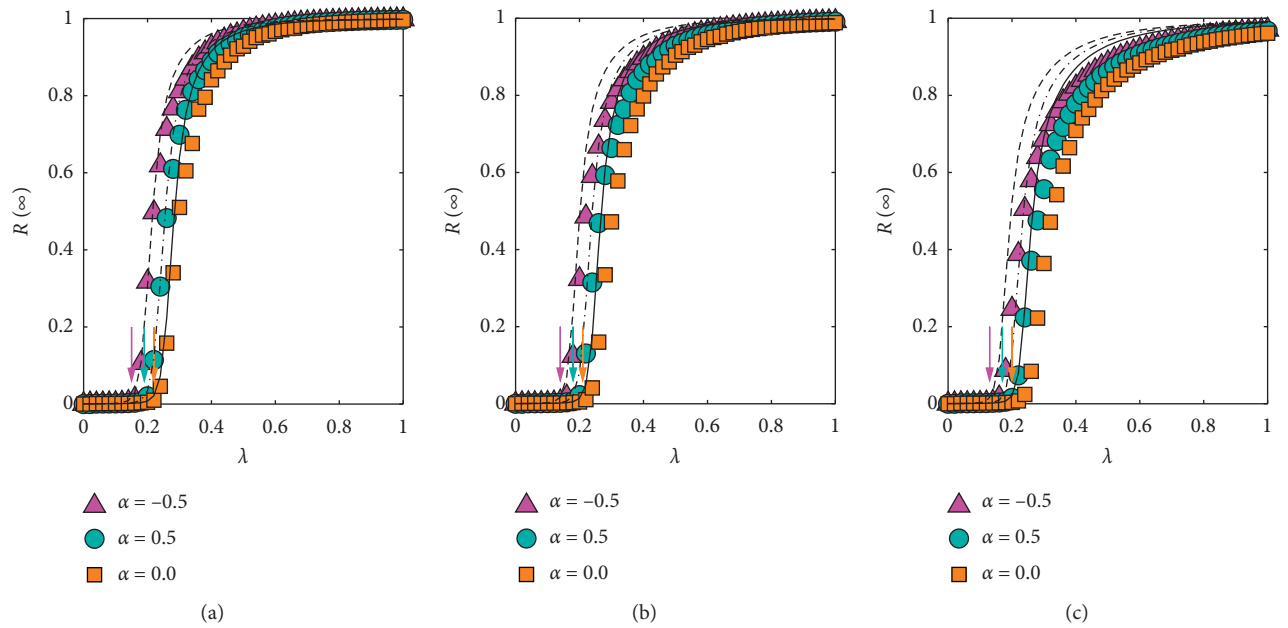

Figure 3: Continued.

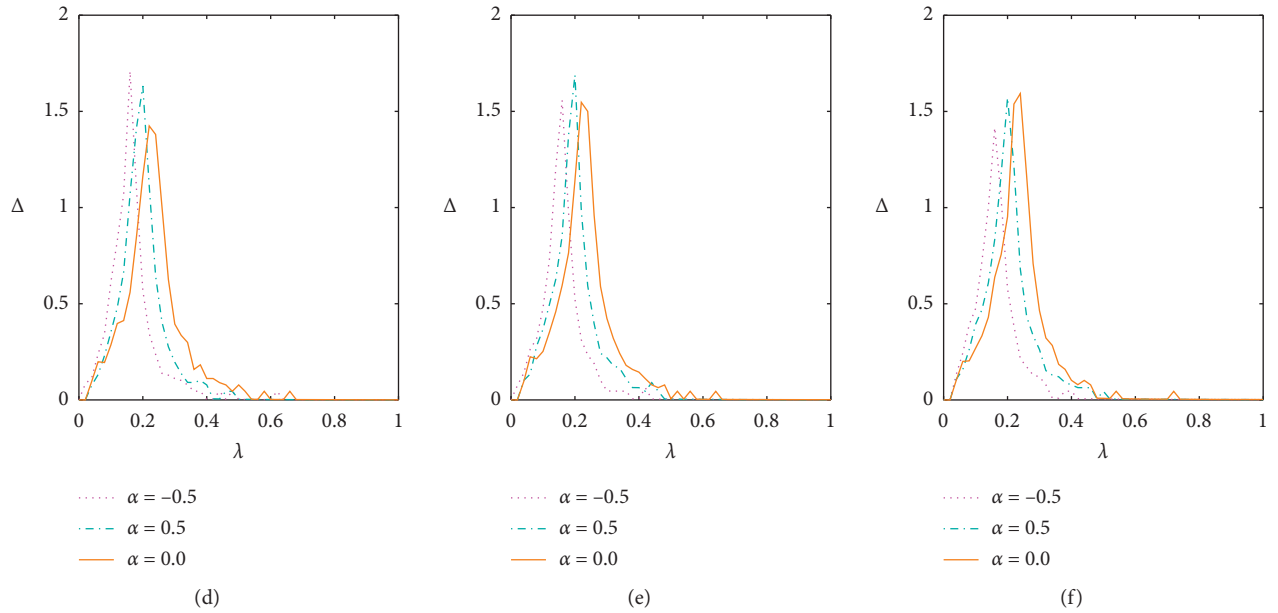

Figure 3: The variation of the outbreak size $R(\infty)$ with the transmission probability λ with different preference selection parameters β. (a) ($\beta = -1$), (b) ($\beta = 0$), and (c) ($\beta = 1$). The symbols and lines are the simulated and theoretical values of $R(\infty)$ in (a)–(c), respectively, where $\alpha = -0.5$ (pink triangles), $\alpha = 0.0$ (orange squares), and $\alpha = 0.5$ (blue-green circles). The arrows are theoretical outbreak threshold. The simulated outbreak threshold Δ as a function of λ with $\beta = -1$ (d), $\beta = 0$ (e), and $\beta = 1$ (f) for the corresponding values of α in (a)–(c), respectively. Another parameter is $f = 0.05$.

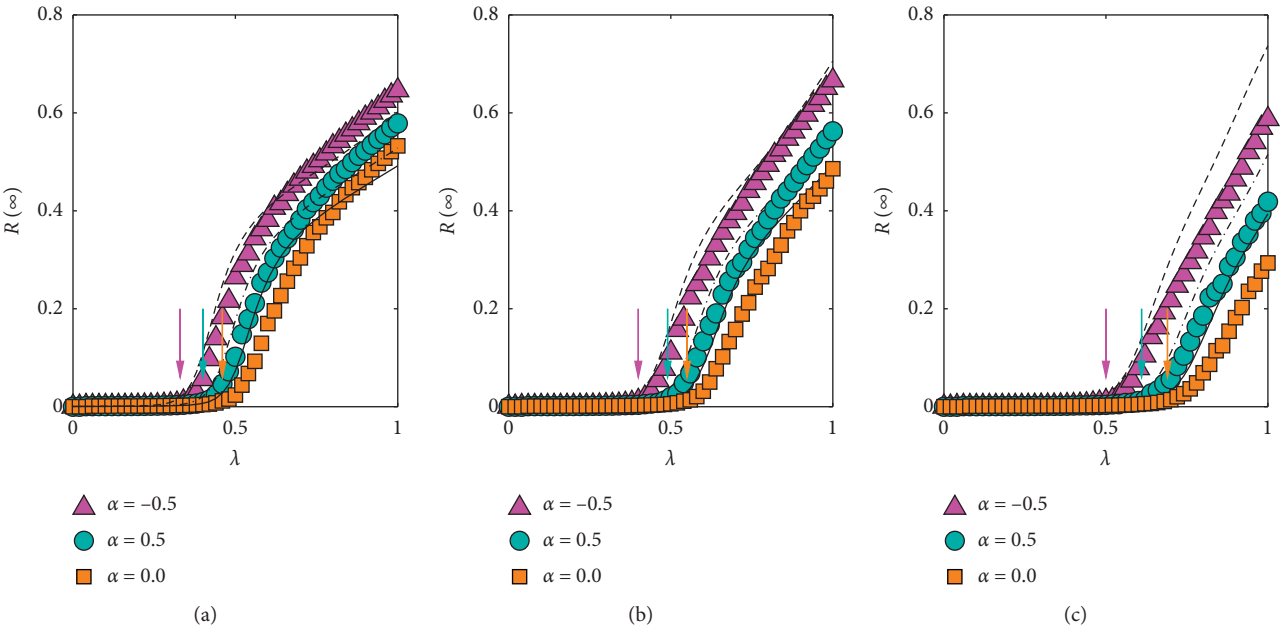

Figure 4: Continued.

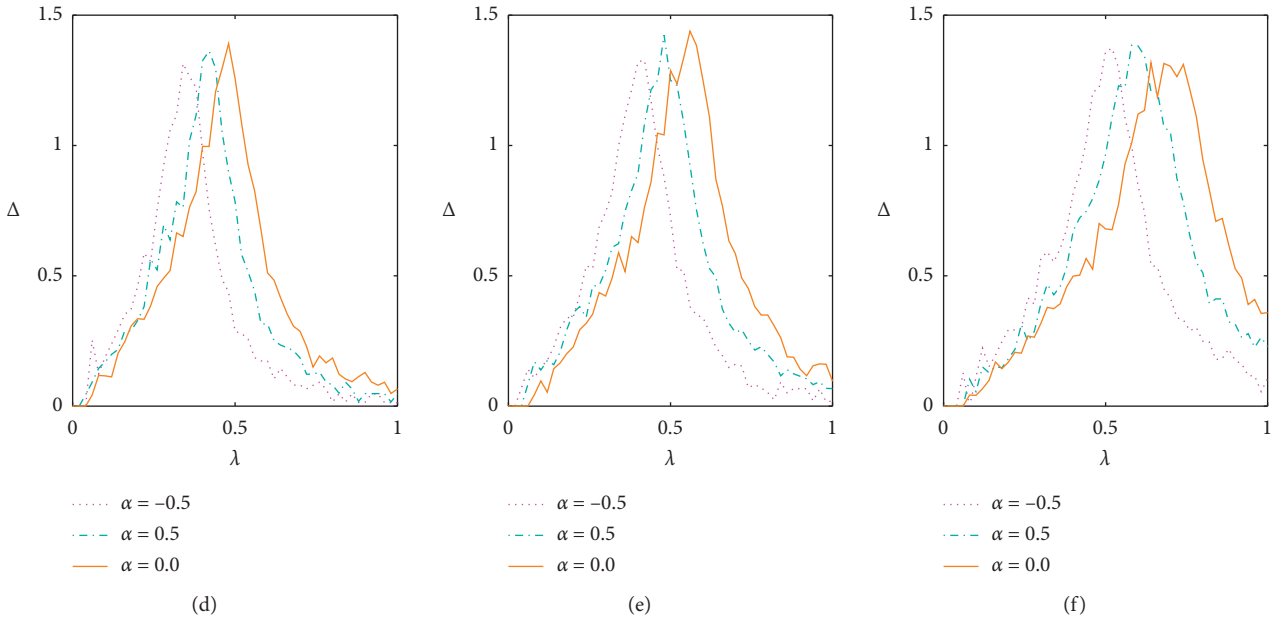

Figure 4: The variation of the outbreak size $R(\infty)$ with the transmission probability λ with different preference selection parameters β. (a) ($\beta = -1$), (b) ($\beta = 0$), and (c) ($\beta = 1$). The symbols and lines are the simulated and theoretical values of $R(\infty)$ in (a)–(c), respectively, where $\alpha = -0.5$ (pink triangles), $\alpha = 0.0$ (orange squares), and $\alpha = 0.5$ (blue-green circles). The arrows are theoretical outbreak threshold. The simulated outbreak threshold Δ as a function of λ with $\beta = -1$ (d), $\beta = 0$ (e), and $\beta = 1$ (f) for the corresponding values of α in (a)–(c), respectively. Another parameter is $f = 0.01$.

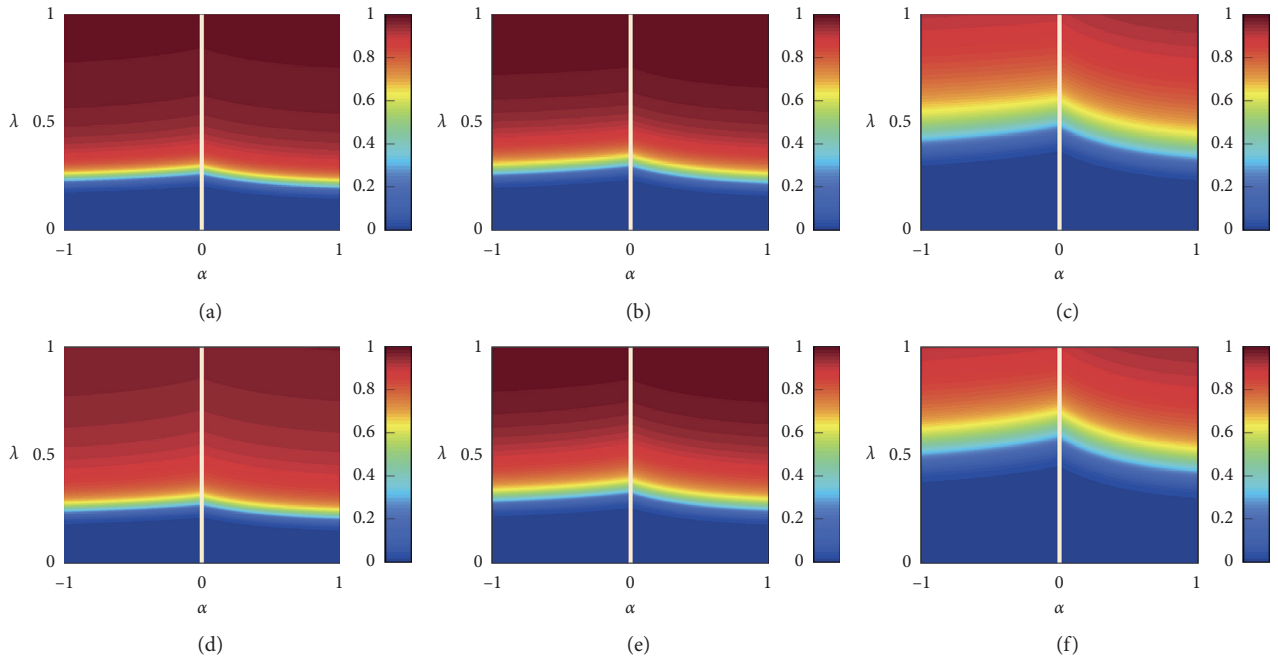

Figure 5: Continued.

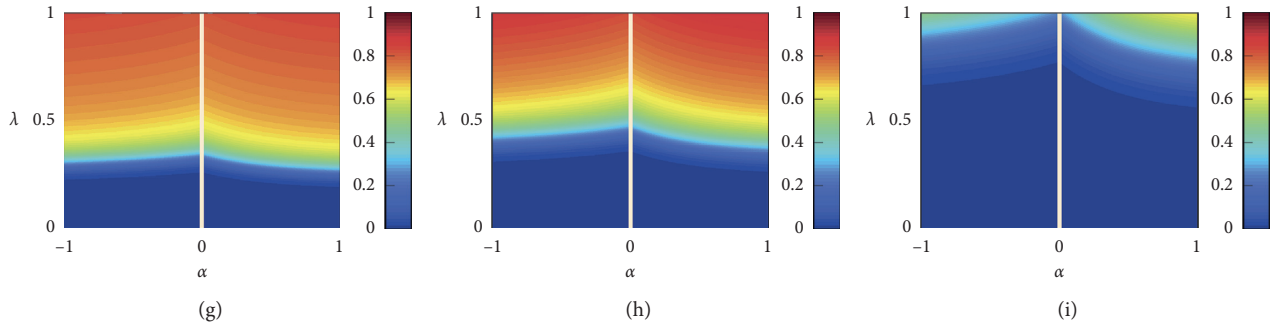

FIGURE 5: The theoretical outbreak size $R(\infty)$ as a function of resource providing parameter α and transmission probability λ on the scale-free network with $\beta = -1$ (a) (d) (g), $\beta = 0$ (b) (e) (h), and $\beta = 1$ (c) (f) (i). (a)–(c) ($f = 0.03$), (d)–(f) ($f = 0.05$), and (g)–(i) ($f = 0.1$). Colors represent the values of $R(\infty)$. The white dotted line in each subgraph indicates the optimal value of $\alpha_{opt} = 0$. Other parameters are $k_{min} = 6$, $k_{max} = 100$, and $\gamma = 3$.

5. Conclusion

In the process of the real epidemic spreading, first of all, the possibility of each node being susceptible to infection is different; that is, each node itself has an inherent infection threshold to reflect the susceptibility of the node. Next, due to the limited energy and time of epidemic disseminators, the process of epidemic transmission is affected. Finally, the resource supporting is determined by the degree of nodes. The above three aspects have a significant impact on the spread and recovery of the epidemic. Previous works have separately studied the influence of three aspects of epidemic dynamics, but no studies have included the three aspects into the same dynamics of epidemic spreading at the same time. Therefore, we proposed a model, including three aspects to study them simultaneously. Besides, we extended the heterogeneous mean-field theory to describe the model. Through theoretical analysis and a large number of numerical simulations, we find that the recovered nodes provide resources uniformly to their infected neighbor nodes, and the epidemic spreading can be suppressed optimally, i.e., the outbreak threshold is maximum, and the outbreak size is minimum for $\alpha = 0.0$ on homogeneous and heterogeneous networks. The change of threshold parameter f and preference selection parameter β has no qualitative change to the above conclusion. The increase of f increases the infection threshold of each node; that is, the susceptibility of the node decreases, thus increasing the outbreak threshold of epidemic spreading and decreasing the outbreak size. The conclusion of this paper can be used as a reference for the suppression of epidemic spreading, and the theory proposed can be applied to other network dynamic processes. For example, uninfected individuals may provide uniform resources and help susceptible individuals who can be contacted. The research in this paper can be extended to more real networks, such as sequential networks and multilayer networks. Finally, our research results may shed some light on studying the critical phenomena on complex networks.

Data Availability

The data used to support the findings of this study are available from the corresponding author upon request.

Conflicts of Interest

The authors declare that they have no conflicts of interest.

Acknowledgments

This work was supported by the National Key Research and Development Program of China (2017YFC-0803903).

References

[1] R. Pastor-Satorras, C. Castellano, P. Van Mieghem, and A. Vespignani, "Epidemic processes in complex networks," *Reviews of Modern Physics*, vol. 87, no. 3, pp. 925–979, 2015.

[2] C. Castellano, S. Fortunato, and V. Loreto, "Statistical physics of social dynamics," *Reviews of Modern Physics*, vol. 81, no. 2, pp. 591–646, 2009.

[3] M. Garetto, W. Gong, and D. Towsley, "Modeling malware spreading dynamics,"vol. 3, pp. 1869–1879, in *Proceedings of the IEEE Twenty-Second Annual Joint Conference of the IEEE Computer and Communications Societies INFOCOM 2003 (IEEE Cat. No. 03CH37428)*, vol. 3, , IEEE, San Francisco, CA, USA, March 2003.

[4] Z. Li, P. Zhu, D. Zhao, Z. Deng, and Z. Wang, "Suppression of epidemic spreading process on multiplex networks via active immunization," *Chaos: An Interdisciplinary Journal of Nonlinear Science*, vol. 29, no. 7, Article ID 073111, 2019.

[5] G. Yan, G. Chen, S. Eidenbenz, and N. Li, "Malware propagation in online social networks: nature, dynamics, and defense implications," in *Proceedings of the 6th ACM Symposium on Information, Computer and Communications Security*, pp. 196–206, Hong Kong, China, March 2011.

[6] R. Pastor-Satorras and A. Vespignani, "Epidemic spreading in scale-free networks," *Physical Review Letters*, vol. 86, no. 14, pp. 3200–3203, 2001.

[7] A. Saumell-Mendiola, M. Á. Serrano, and M. Boguná, "Epidemic spreading on interconnected networks," *Physical Review E*, vol. 86, no. 2, Article ID 026106, 2012.

[8] P. Zhu, X. Wang, S. Li, Y. Guo, and Z. Wang, "Investigation of epidemic spreading process on multiplex networks by incorporating fatal properties," *Applied Mathematics and Computation*, vol. 359, pp. 512–524, 2019.

[9] M. Boguá, R. Pastor-Satorras, and A. Vespignani, "Epidemic spreading in complex networks with degree correlations," in *Statistical Mechanics of Complex Networks*, pp. 127–147, Springer, Berlin, Germany, 2003.

[10] J. W. Mickens and B. D. Noble, "Modeling epidemic spreading in mobile environments," in *Proceedings of the 4th ACM Workshop on Wireless Security*, pp. 77–86, Cologne, Germany, September 2005.

[11] J. T. Matamalas, S. Gómez, and A. Arenas, "Abrupt phase transition of epidemic spreading in simplicial complexes," *Physical Review Research*, vol. 2, no. 1, Article ID 012049, 2020.

[12] M. Li, M. Wang, S. Xue, and J. Ma, "The influence of awareness on epidemic spreading on random networks," *Journal of Theoretical Biology*, vol. 486, Article ID 110090, 2020.

[13] C. Buono and L. A. Braunstein, "Immunization strategy for epidemic spreading on multilayer networks," *EPL (Europhysics Letters)*, vol. 109, no. 2, Article ID 26001, 2015.

[14] M. Salehi, R. Sharma, M. Marzolla, M. Magnani, P. Siyari, and D. Montesi, "Spreading processes in multilayer networks," *IEEE Transactions on Network Science and Engineering*, vol. 2, no. 2, pp. 65–83, 2015.

[15] M. De Domenico, C. Granell, M. A. Porter, and A. Arenas, "The physics of spreading processes in multilayer networks," *Nature Physics*, vol. 12, no. 10, p. 901, 2016.

[16] L. A. Zuzek, H. E. Stanley, and L. A. Braunstein, "Epidemic model with isolation in multilayer networks," *Scientific Reports*, vol. 5, Article ID 12151, 2015.

[17] D. Zhao, L. Li, H. Peng, Q. Luo, and Y. Yang, "Multiple routes transmitted epidemics on multiplex networks," *Physics Letters A*, vol. 378, no. 10, pp. 770–776, 2014.

[18] P. Zhu, X. Song, L. Liu, Z. Wang, and J. Han, "Stochastic analysis of multiplex Boolean networks for understanding epidemic propagation," *IEEE Access*, vol. 6, pp. 35292–35304, 2018.

[19] Z. Wang, D.-W. Zhao, L. Wang, G.-Q. Sun, and Z. Jin, "Immunity of multiplex networks via acquaintance vaccination," *EPL (Europhysics Letters)*, vol. 112, no. 4, Article ID 48002, 2015.

[20] D. Zhao, L. Wang, Z. Wang, and G. Xiao, "Virus propagation and patch distribution in multiplex networks: modeling, analysis, and optimal allocation," *IEEE Transactions on Information Forensics and Security*, vol. 14, no. 7, pp. 1755–1767, 2019.

[21] J. T. Davis, N. Perra, Q. Zhang, Y. Moreno, and A. Vespignani, "Phase transitions in information spreading on structured populations," *Nature Physics*, vol. 16, no. 5, pp. 590–596, 2020.

[22] P. Shu, W. Wang, M. Tang, P. Zhao, and Y.-C. Zhang, "Recovery rate affects the effective epidemic threshold with synchronous updating," *Chaos*, vol. 26, no. 2, Article ID 063108, 2016.

[23] M. Starnini, J. P. Gleeson, and M. Boguñá, "Equivalence between non-Markovian and Markovian dynamics in epidemic spreading processes," *Physical Review Letters*, vol. 118, no. 12, Article ID 128301, 2017.

[24] P. Van Mieghem and R. Van de Bovenkamp, "Non-Markovian infection spread dramatically alters the susceptible-infected-susceptible epidemic threshold in networks," *Physical Review Letters*, vol. 110, no. 10, Article ID 108701, 2013.

[25] M. Boguná, L. F. Lafuerza, R. Toral, and M. Á. Serrano, "Simulating non-Markovian stochastic processes," *Physical Review E*, vol. 90, no. 4, Article ID 042108, 2014.

[26] I. Scholtes, N. Wider, R. Pfitzner, A. Garas, C. J. Tessone, and F. Schweitzer, "Causality-driven slow-down and speed-up of diffusion in non-Markovian temporal networks," *Nature Communications*, vol. 5, no. 1, pp. 1–9, 2014.

[27] N. Sherborne, J. C. Miller, K. B. Blyuss, and I. Z. Kiss, "Mean-field models for non-Markovian epidemics on networks," *Journal of Mathematical Biology*, vol. 76, no. 3, pp. 755–778, 2018.

[28] B. Karrer and M. E. Newman, "Message passing approach for general epidemic models," *Physical Review E*, vol. 82, no. 1, Article ID 016101, 2010.

[29] G. F. de Arruda, G. Petri, F. A. Rodrigues, and Y. Moreno, "Impact of the distribution of recovery rates on disease spreading in complex networks," *Physical Review Research*, vol. 2, no. 1, Article ID 013046, 2020.

[30] T. Philipson, "Economic epidemiology and infectious diseases," *Nber Working Papers*, vol. 1, pp. 1761–1799, 1999.

[31] X. Chen, T. Zhou, L. Feng et al., "Nontrivial resource requirement in the early stage for containment of epidemics," *Physical Review E*, vol. 100, no. 3, Article ID 032310, 2019.

[32] X. Chen, R. Wang, M. Tang, S. Cai, H. E. Stanley, and L. A. Braunstein, "Suppressing epidemic spreading in multiplex networks with social-support," *New Journal of Physics*, vol. 20, no. 1, Article ID 013007, 2018.

[33] X. Chen, W. Wang, S. Cai, H. E. Stanley, and L. A. Braunstein, "Optimal resource diffusion for suppressing disease spreading in multiplex networks," *Journal of Statistical Mechanics: Theory and Experiment*, vol. 2018, no. 5, Article ID 053501, 2018.

[34] X.-L. Chen, R.-J. Wang, C. Yang, and S.-M. Cai, "Hybrid resource allocation and its impact on the dynamics of disease spreading," *Physica A: Statistical Mechanics and Its Applications*, vol. 513, pp. 156–165, 2019.

[35] X.-L. Chen, S.-M. Cai, M. Tang, W. Wang, T. Zhou, and P.-M. Hui, "Controlling epidemic outbreak based on local dynamic infectiousness on complex networks," *Chaos: An Interdisciplinary Journal of Nonlinear Science*, vol. 28, no. 12, Article ID 123105, 2018.

[36] S. Zhang, T. Wu, W. Wang, and T. Lin, "Irreversible contact process on complex networks with dynamical recovery probability," *Physica A: Statistical Mechanics and Its Applications*, vol. 527, Article ID 121336, 2019.

[37] J. C. Miller, "Epidemic size and probability in populations with heterogeneous infectivity and susceptibility," *Physical Review E*, vol. 76, no. 1, Article ID 010101, 2007.

[38] D. J. Watts, "A simple model of global cascades on random networks," *Proceedings of the National Academy of Sciences*, vol. 99, no. 9, pp. 5766–5771, 2002.

[39] R. Yang, T. Zhou, Y.-B. Xie, Y.-C. Lai, and B.-H. Wang, "Optimal contact process on complex networks," *Physical Review E*, vol. 78, no. 6, Article ID 066109, 2008.

[40] R. Yang, L. Huang, and Y.-C. Lai, "Selectivity-based spreading dynamics on complex networks," *Physical Review E*, vol. 78, no. 2, Article ID 026111, 2008.

[41] M. Catanzaro, M. Boguná, and R. Pastor-Satorras, "Generation of uncorrelated random scale-free networks," *Physical review e*, vol. 71, no. 2, Article ID 027103, 2005.

[42] P. S. Dodds and D. J. Watts, "A generalized model of social and biological contagion," *Journal of Theoretical Biology*, vol. 232, no. 4, pp. 587–604, 2005.

[43] D. Centola, "The spread of behavior in an online social network experiment," *Science*, vol. 329, no. 5996, pp. 1194–1197, 2010.

[44] H. P. Young, "The dynamics of social innovation," *Proceedings of the National Academy of Sciences*, vol. 108, no. 4, pp. 21285–21291, 2011.

[45] S. H. Strogatz, *Nonlinear Dynamics and Chaos: With Applications to Physics, Biology, Chemistry, and Engineering*, Westview Press, Boulder, CO, USA, 2014.

[46] P. Shu, W. Wang, M. Tang, and Y. Do, "Numerical identification of epidemic thresholds for susceptible-infected-recovered model on finite-size networks," *Chaos*, vol. 25, no. 6, Article ID 063104, 2015.